



OPEN ACCESS

EDITED BY

Constantino Carlos Reyes-Aldasoro,
City University of London, United Kingdom

REVIEWED BY

Jesús Silva-Rodríguez,
Institute of Biomedicine of Seville (IBIS), Spain
Ming-Chun Yu,
Cardinal Tien Hospital, Taiwan

*CORRESPONDENCE

Guoguang Zhao
✉ ggzhao@vip.sina.com
Wen Qin
✉ wayne.wenqin@gmail.com
Yongzhi Shan
✉ shanyongzhi@xwhosp.org

RECEIVED 04 February 2023

ACCEPTED 03 May 2023

PUBLISHED 30 May 2023

CITATION

Huang Y, Shan Y, Qin W and Zhao G (2023)
Apolipoprotein E ϵ 4 accelerates the
longitudinal cerebral atrophy in open access
series of imaging studies-3 elders without
dementia at enrollment.

Front. Aging Neurosci. 15:1158579.

doi: 10.3389/fnagi.2023.1158579

COPYRIGHT

© 2023 Huang, Shan, Qin and Zhao. This is an
open-access article distributed under the terms
of the [Creative Commons Attribution License
\(CC BY\)](https://creativecommons.org/licenses/by/4.0/). The use, distribution or reproduction
in other forums is permitted, provided the
original author(s) and the copyright owner(s)
are credited and that the original publication in
this journal is cited, in accordance with
accepted academic practice. No use,
distribution or reproduction is permitted which
does not comply with these terms.

Apolipoprotein E ϵ 4 accelerates the longitudinal cerebral atrophy in open access series of imaging studies-3 elders without dementia at enrollment

Yuda Huang¹, Yongzhi Shan^{1*}, Wen Qin^{2*} and
Guoguang Zhao^{1,3,4*}

¹Department of Neurosurgery, Xuanwu Hospital Capital Medical University, Beijing, China, ²Department of Radiology, Tianjin Medical University General Hospital, Tianjin, China, ³Clinical Research Center for Epilepsy Capital Medical University, Beijing, China, ⁴Beijing Municipal Geriatric Medical Research Center, Beijing, China

Introduction: Early studies have reported that APOE is strongly associated with brain atrophy and cognitive decline among healthy elders and Alzheimer's disease (AD). However, previous research has not directly outlined the modulation of APOE on the trajectory of cerebral atrophy with aging during the conversion from cognitive normal (CN) to dementia (CN2D).

Methods: This study tried to elucidate this issue from a voxel-wise whole-brain perspective based on 416 qualified participants from a longitudinal OASIS-3 neuroimaging cohort. A voxel-wise linear mixed-effects model was applied for detecting cerebrum regions whose nonlinear atrophic trajectories were driven by AD conversion and to elucidate the effect of APOE variants on the cerebral atrophic trajectories during the process.

Results: We found that CN2D participants had faster quadratically accelerated atrophy in bilateral hippocampi than persistent CN. Moreover, APOE ϵ 4 carriers had faster-accelerated atrophy in the left hippocampus than ϵ 4 noncarriers in both CN2D and persistent CN, and CN2D ϵ 4 carriers an noncarriers presented a faster atrophic speed than CN ϵ 4 carriers. These findings could be replicated in a sub-sample with a tough match in demographic information.

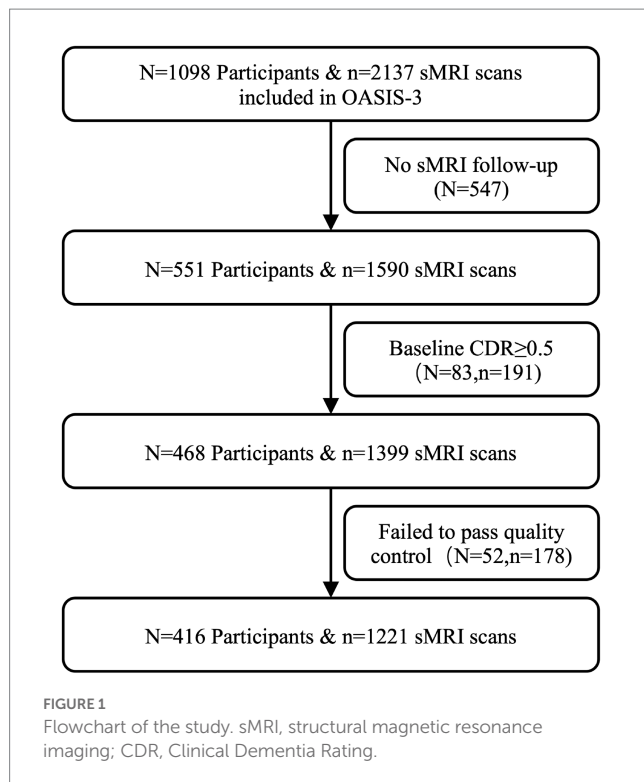
Discussion: Our findings filled the gap that APOE ϵ 4 accelerates hippocampal atrophy and the conversion from normal cognition to dementia.

KEYWORDS

Alzheimer's disease, cerebral atrophic, apolipoprotein E, aging, dementia

1. Introduction

Alzheimer's disease (AD) is a progressive neurodegenerative disease causing dementia (Scheltens et al., 2021). Apolipoprotein E (APOE) plays a significant role during the conversion from cognitive normal (CN) to AD through regulating Amyloid- β peptide (A β) metabolism, aggregation, and deposition (Kanekiyo et al., 2014; Mahoney-Sanchez et al., 2016; Belloy et al., 2019), in which ϵ 4 allele of APOE is widely acknowledged as the strongest genetic risk variant for AD (Gharbi-Meliani et al., 2021; Serrano-Pozo et al., 2021).



Brain atrophy is intensely associated with the development and progression of AD (Buckner, 2004). Structural magnetic resonance imaging (sMRI) provides an accessible and non-invasive way to monitor brain atrophy with high spatial resolution and tissue differentiation (Pini et al., 2016; Rathore et al., 2017). Hence, sMRI provides a promising tool to clarify the relationships between brain atrophy and AD conversion (Jack et al., 2005), and many sMRI-based neuroimaging studies have made great contributions to AD diagnosis (Arbabshirani et al., 2017; Lian et al., 2020), as well as clinical progression prediction and monitoring (Tabatabaei-Jafari et al., 2019; Veitch et al., 2019).

APOE $\epsilon 4$ allele association with brain atrophy and cognitive decline has been reported in healthy aging individuals and dementia patients (Saeed et al., 2021). Moreover, cross-sectional (Burggren et al., 2008; Regy et al., 2022) and longitudinal (Lu et al., 2011; Squarzone et al., 2018) studies demonstrated that $\epsilon 4$ -carriers exhibit severe hippocampus atrophy during aging in CN individuals. Longitudinal studies also disclosed that $\epsilon 4$ -carriers present greater risks of hippocampal gray matter atrophy among mild cognitive impairment (MCI) and dementia patients (Racine et al., 2018; Abushakra et al., 2020). Gray matter atrophies in several cerebral regions, including the caudate, hippocampus, and insula, were reported to correlate with APOE allele during the conversion from MCI to AD (Wei et al., 2022). However, no study has directly outlined the modulation of APOE on the trajectory of cerebral atrophy through the whole process from normal cognition to dementia. Besides, most early studies only focused on candidate brain regions, and studies illustrating the effect of APOE on cerebral atrophy from the whole brain's voxel-wise perspective are still limited and remain to be further discussed.

Thus, this study aims to draw full trajectory maps of cerebral gray matter atrophy in the elderly with and without APOE $\epsilon 4$ variant from the normal cognition stage to dementia. We hypothesized that APOE $\epsilon 4$ would accelerate the atrophy of multiple cerebral regions during

conversion from normal cognition (CN) to dementia (CN2D) and aimed to seek specific brain regions relative to AD conversion using a voxel-wise method and explored the influence of APOE variants on their atrophic trajectories. First, we investigate the effect of groups (persistent CN versus CN2D) on the gray matter atrophic trajectories with aging to seek specific target areas relative to AD conversion. Moreover, we explored the influence of APOE variants on the atrophic trajectories of target brain regions from CN to dementia stages.

2. Materials and methods

2.1. Participants

Participants enrolled in the study were acquired from the Open Access Series of Imaging Studies-3 (OASIS-3) database,¹ which includes neuroimaging, clinical, cognitive, and biomarker data of 609 CN adults and 489 participants aged 42 to 95 years at different stages of cognitive decline. All participants were consented into Knight ADRC-related projects following procedures approved by the Institutional Review Board of Washington University School of Medicine in accordance with the Declaration of Helsinki.

Firstly, we included subjects with at least 2 longitudinal sMRIs and corresponding clinical follow-up data, resulting in 551 participants and 1,590 sMRI scans. Secondly, we selected participants whose Clinical Dementia Rating (CDR)=0 at baseline (removing 83 participants and 191 sMRI scans). Third, 178 sMRI scans of 52 participants were excluded because of poor imaging quality. Moreover, we categorized participants whose cognition maintained normal during all follow-up time points as the CN group and defined subjects who converted to dementia (CDR \geq 0.5) during follow-ups as the CN2D group. Additionally, subjects carrying at least one APOE $\epsilon 4$ allele copy were defined as APOE $\epsilon 4$ carriers, while subjects with APOE genotype of $\epsilon 3/\epsilon 3$, $\epsilon 3/\epsilon 2$, or $\epsilon 2/\epsilon 2$ were recognized as APOE $\epsilon 4$ noncarriers. Finally, 416 subjects consisting of 54 CN2D (22 APOE $\epsilon 4$ carriers and 32 APOE $\epsilon 4$ noncarriers, 150scans) and 362 CN (107 $\epsilon 4$ carriers and 255 $\epsilon 4$ noncarriers, 1071scans) were included in the final analysis. The flowchart of participant enrollment is presented in Figure 1. Considering the mismatch in sample size and demographics between CN and CN2D groups, we additionally took CN2D subjects as the reference to match the CN participant with the same gender and age distributions.

2.2. Image preprocessing

The T1 weighted sMRI data of each subject were preprocessed using a longitudinal pipeline based on CAT12 toolbox² for SPM12 software.³ Firstly, follow-up sMRI scans of every participant were rigidly co-registered to his/her baseline images. Individual-specific average T1W images were generated based on their longitudinal follow-up images. Then the average images were normalized to Montreal Neurological Institute (MNI) space using a DARTEL algorithm (Ashburner, 2007). The co-registered sMRI images of each

¹ www.oasis-brains.org

² <https://neuro-jena.github.io/cat12-help/cat.html>

³ <https://www.fil.ion.ucl.ac.uk/spm/software/spm12/>

scan were segmented into gray matter (GM), white matter (WM), and cerebrospinal fluid (CSF). Each GM map was transformed into the MNI space using the subject-specific deformation field parameters based on average images, and was modulated by the Jacobian determinants to calculate the gray matter volume (GMV). The total intracranial volume (TIV) was also generated for further statistical analysis. Finally, GMV maps were all smoothed according to an 8 mm³ full-width at half-maximum (FWHM) Gaussian kernel (Radua et al., 2014). Additionally, the Automated Anatomical Labeling (AAL) atlas (Tzourio-Mazoyer et al., 2002) with 90 cerebral regions was applied to extract GMV from each subjects' sMRI scans.

2.3. Statistical analyzes

2.3.1. Cerebral atrophic trajectories from CN to dementia conversion

In order to identify brain regions whose atrophic trajectories were specific for CN2D progression rather than consistent CN, a voxel-wise linear mixed-effects (LME) model was first introduced with GMV as the dependent variable, linear and quadratic interaction between age and group (CN2D vs. CN) as interested fixed-effects, subjects as random effects, and gender and TIV as confounding fixed-effect covariates. LME could simulate both fixed and random effects and accommodate irregular follow-up intervals with missing time nodes [Bernal-Rusiel et al., 2013; Model (1)].

$$GMV = \beta_1 CN + \beta_2 (CN \times Age) + \beta_3 (CN \times Age^2) + \beta_4 CN2D + \beta_5 (CN2D \times Age) + \beta_6 (CN2D \times Age^2) + \beta_7 TIV + \beta_8 Gender + (1 + Age|Subject) \quad (1)$$

Age and Age² represent the linear and quadratic terms of age, respectively.

Intergroup differences in nonlinear GMV-age association were estimated based on joint (or multiple) hypothesis testing using the F-statistics (Shaffer, 1995; Hanck et al., 2019). Joint hypothesis testing combines multiple null hypotheses into one single test (for example, we assumed the linear and quadratic interaction terms between age and group are zero), which will return an F-statistic for this joint null hypothesis. Brain regions were regarded significant if the statistics persist after family-wise error (FWE) correction for multiple comparisons ($p < 0.05$) and cluster size larger than 20 voxels. The voxel-wise interaction between age and group was carried out using the flexible factor model design embedded in SPM12.

For brain regions showing significant age-group interaction, we extracted the mean GMV of each region of interest (ROI) to outline the atrophy trajectory as a function of age in CN and CN2D, respectively. The same post-hoc LME model (Model 1) was applied to each ROI to fit the nonlinear association between GMV and age in each group, and the joint hypothesis testing was used to test the significance of model fitting ($p < 0.05$).

2.3.2. Effects of APOE $\epsilon 4$ on cerebral atrophic trajectories from CN to dementia conversion

To test the influence of APOE variants on longitudinal cerebral atrophy with aging, we secondly carried out another voxel-wise LME

statistic with GMV as the dependent variable, linear and quadratic interaction between age and APOE variants ($\epsilon 4$ carriers vs. noncarriers) as interested fixed-effects, subjects as random effects, and gender and TIV as confounding fixed-effect covariates (Model 2). Similarly, a joint hypothesis testing was used to estimate the differences in nonlinear GMV-age association between the $\epsilon 4$ carriers and noncarriers [$p < 0.05$, voxel-wise FWE correction, with cluster-size > 20 voxels; Model (2)].

$$GMV = \beta_1 \epsilon 4 \text{ carrier} + \beta_2 (\epsilon 4 \text{ carrier} \times Age) + \beta_3 (\epsilon 4 \text{ carrier} \times Age^2) + \beta_4 \epsilon 4 \text{ non-carrier} + \beta_5 (\epsilon 4 \text{ noncarrier} \times Age) + \beta_6 (\epsilon 4 \text{ noncarrier} \times Age^2) + \beta_7 TIV + \beta_8 Gender + (1 + Age|Subject) \quad (2)$$

Besides, we extracted the average GMV of each ROI showing significant APOE effects. A *post hoc* analysis based on LME models was used to outline the atrophy trajectory under the effect of age in APOE $\epsilon 4$ carriers and noncarriers in all participants [Model (2)], and in CN and CN2D, respectively [joint hypothesis testing, $p < 0.05$; Model (3)]. A joint hypothesis test was applied to estimate the nonlinear association between GMV and age in each group and APOE variant, and to test GMV-age association differences between APOE $\epsilon 4$ carriers and noncarriers in each group ($p < 0.05$).

$$GMV = \beta_1 CN \& \epsilon 4 \text{ carrier} + \beta_2 (CN \& \epsilon 4 \text{ carrier} \times Age) + \beta_3 (CN \& \epsilon 4 \text{ carrier} \times Age^2) + \beta_4 CN \& \epsilon 4 \text{ noncarrier} + \beta_5 (CN \& \epsilon 4 \text{ noncarrier} \times Age) + \beta_6 (CN \& \epsilon 4 \text{ noncarrier} \times Age^2) + \beta_7 CN2D \& \epsilon 4 \text{ carrier} + \beta_8 (CN2D \& \epsilon 4 \text{ carrier} \times Age) + \beta_9 (CN2D \& \epsilon 4 \text{ carrier} \times Age^2) + \beta_{10} CN2D \& \epsilon 4 \text{ noncarrier} + \beta_{11} (CN2D \& \epsilon 4 \text{ noncarrier} \times Age) + \beta_{12} (CN2D \& \epsilon 4 \text{ noncarrier} \times Age^2) + \beta_{13} TIV + \beta_{14} Gender + (1 + Age|Subject) \quad (3)$$

2.3.3. Demographic statistics

Our study analyzed demographic data using the Statistical Package for the Social Sciences version 26.0 (SPSS). Two-sample sample *t*-test (normal distribution) or Mann-Whitney U test (non-normal distribution) was used to compare differences in continuous variables between the CN and CN2D or between $\epsilon 4$ carriers and $\epsilon 4$ noncarriers ($p < 0.05$). Categorical variables, including gender and APOE status, were examined by the Chi-square test ($p < 0.05$). In addition, the consistent effect size between two separate groups was measured by calculating Cohen's *d* value.

3. Results

3.1. Demographic characteristics

The demographic characteristics and cognitive status of all the enrolled participants are summarized in Table 1. There was no statistical difference in baseline age at the first sMRI scan (two-sample *t*-test, $t = 1.903$, $p = 0.058$), follow-up durations (Mann-Whitney U

TABLE 1 Demographic information of all enrolled participants.

	No. Subjects	Baseline age (years)	Follow-up duration (days)	Gender (M/F)	Follow-up times	Baseline MMSE	End MMSE
$\epsilon 4$ _Carrier	129	65.62 ± 9.27	2256.67 ± 1421.67	50/79	2.81 ± 1.14	29.03 ± 1.42	28.95 ± 1.52
$\epsilon 4$ _non-Carrier	287	67.49 ± 9.18	2442.55 ± 1413.25	117/170	3.00 ± 1.25	29.17 ± 1.05	29.03 ± 1.81
Statistics		$t = -1.903^*$	$Z = -1.355^*$	$\chi^2 = 0.149^{\circ}$	$Z = -1.439^*$	$Z = -0.172^*$	$Z = -0.606^*$
Cohen's d values		$d = 0.203$	$d = 0.131$		$d = 0.159$	$d = 0.112$	$d = 0.048$
p values		$p = 0.058$	$p = 0.176$	$p = 0.699$	$p = 0.150$	$p = 0.864$	$p = 0.544$
CN2D	54	73.12 ± 7.73	2224.85 ± 1201.69	30/24	2.80 ± 1.27	28.59 ± 1.60	27.52 ± 3.52
CN	362	65.98 ± 9.09	2408.78 ± 1446.05	137/225	2.96 ± 1.21	29.20 ± 1.09	29.23 ± 1.10
Statistics		$t = 5.483^*$	$Z = -0.751^*$	$\chi^2 = 6.134^{\circ}$	$Z = -1.348^*$	$Z = -2.953^*$	$Z = -5.625^*$
Cohen's d values		$d = 0.846$	$d = 0.138$		$d = 0.129$	$d = 0.446$	$d = 0.656$
p values		$p < 0.001$	$p = 0.453$	$p = 0.013$	$p = 0.178$	$p = 0.003$	$p < 0.001$

^{*} Mann-Whitney U test; ^{*} Two-sample t -test; [°] Chi-square test. CN, persistent cognitive normal; CN2D, cognitive normal to dementia; sMRI, structural magnetic resonance imaging; MMSE, mini-mental state examination.

TABLE 2 Demographic information of matched participants.

	No. subjects	Baseline age (years)	Follow-up duration (days)	Gender (M/F)	Follow-up times	Baseline MMSE	End MMSE
$\epsilon 4$ _Carrier	37	71.96 ± 8.71	2231.84 ± 1575.76	22/15	2.59 ± 1.04	28.41 ± 1.95	28.05 ± 2.03
$\epsilon 4$ _non-Carrier	71	73.71 ± 7.11	2459.73 ± 1408.91	38/33	2.83 ± 1.13	28.86 ± 1.22	28.38 ± 3.03
Statistics		$t = -1.124^*$	$Z = -1.291^*$	$\chi^2 = 0.347^{\circ}$	$Z = -1.164^*$	$Z = -0.726^*$	$Z = -1.557^*$
Cohen's d values		$d = 0.220$	$d = 0.152$		$d = 0.221$	$d = 0.278$	$d = 0.128$
p values		$p = 0.264$	$p = 0.197$	$p = 0.556$	$p = 0.244$	$p = 0.468$	$p = 0.120$
CN2D	54	73.12 ± 7.73	2224.85 ± 1201.69	30/24	2.78 ± 1.24	28.59 ± 1.60	27.52 ± 3.52
CN	54	73.10 ± 7.74	2538.46 ± 1684.63	30/24	2.72 ± 0.96	28.81 ± 1.44	29.02 ± 1.21
Statistics		$t = 0.018^*$	$Z = -0.771^*$	$\chi^2 = 0^{\circ}$	$Z = -0.157^*$	$Z = -0.420^*$	$Z = -3.181^*$
Cohen's d values		$d = 0.003$	$d = 0.214$		$d = 0.054$	$d = 0.145$	$d = 0.570$
p values		$p = 0.986$	$p = 0.441$	$p = 1.000$	$p = 0.875$	$p = 0.674$	$p = 0.001$

^{*} Mann-Whitney U test; ^{*} Two-sample t -test; [°] Chi-square test. CN, persistent cognitive normal; CN2D, cognitive normal to dementia; sMRI, structural magnetic resonance imaging; MMSE, mini-mental state examination.

test, $Z = -1.355$, $p = 0.176$), number of sMRI scans per subject (Mann-Whitney U test, $Z = -1.439$, $p = 0.150$), baseline MMSE score (Mann-Whitney U test, $Z = -0.172$, $p = 0.864$), MMSE score by the end of follow-up (Mann-Whitney U test, $Z = -0.606$, $p = 0.544$), and gender (Chi-square test, $\chi^2 = 0.149$, $p = 0.699$) between $\epsilon 4$ carriers and $\epsilon 4$ noncarriers. CN2D patients presented a higher baseline age (two-sample t -test, $t = 5.483$, $p < 0.001$), worse cognitive status at the baseline (Mann-Whitney U test, $Z = -2.953$, $p = 0.003$), and at the end of follow-up (Mann-Whitney U test, $Z = -5.625$, $p < 0.001$) than CN subjects. There was no significant difference between CN and CN2D in follow-up durations (Mann-Whitney U test, $Z = -0.751$, $p = 0.453$), number of sMRI scans per subject (Mann-Whitney U test, $Z = -1.348$, $p = 0.178$). There were statistical differences between CN and CN2D in gender (Chi-square test, $\chi^2 = 6.134$, $p = 0.013$).

In the matched validation set, CN2D and CN participants showed no statistical difference in baseline age (two-sample t -test, $t = 0.018$, $p = 0.986$), follow-up durations (Mann-Whitney U test, $Z = -0.771$, $p = 0.441$), number of sMRI scans per subject (Mann-Whitney U test, $Z = -0.157$, $p = 0.875$), MMSE score at baseline (Mann-Whitney U test, $Z = -0.420$, $p = 0.674$), and gender (Chi-square test, $\chi^2 = 0$,

$p = 1.000$), except for that CN2D had a lower MMSE score by the end of follow-up than the CN (Mann-Whitney U test, $Z = -3.181$, $p = 0.001$; Table 2).

3.2. Cerebral atrophic trajectories differences between CN2D and CN

The voxel-wise LME model identified significant differences in nonlinear GMV atrophy following aging between all CN2D and CN participants, especially in the bilateral hippocampus, insula, post-cingulate cortex (PCC), and caudate ($p < 0.05$, voxel-wise FWE correction; Figure 2A). In the validation dataset with matched sub-samples, we also observed significant differences in GMV atrophic trajectory with aging in the bilateral hippocampi between the CN2D and CN participants (Figure 2B). ROI-wise *post hoc* analysis based on significant voxels identified by the voxel-wise LME model difference demonstrated a faster accelerated GMV atrophy in the bilateral hippocampus in CN2D than the persistent CN (left hippocampus: $F = 60.179$, $p < 0.001$; right hippocampus: $F = 36.359$,

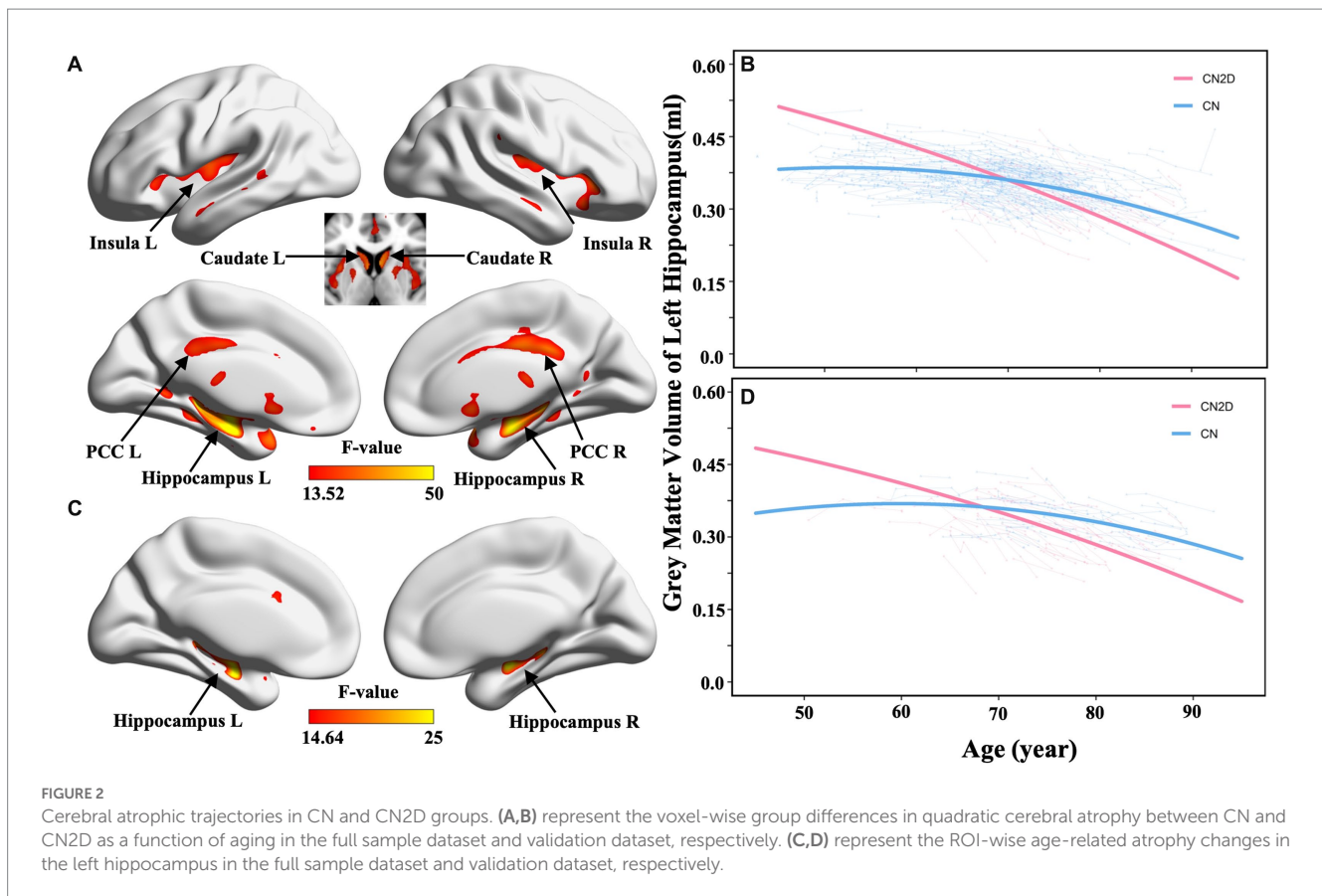


FIGURE 2

Cerebral atrophic trajectories in CN and CN2D groups. (A,B) represent the voxel-wise group differences in quadratic cerebral atrophy between CN and CN2D as a function of aging in the full sample dataset and validation dataset, respectively. (C,D) represent the ROI-wise age-related atrophy changes in the left hippocampus in the full sample dataset and validation dataset, respectively.

$p < 0.001$; Figure 2C; Supplementary Figure S1A), and was validated by the matched sub-sample (left hippocampus: $F = 31.843$, $p < 0.001$; right hippocampus: $F = 21.565$, $p < 0.001$; Figure 2D; Supplementary Figure S1B). For ROI-wise analysis based on AAL atlas, we similarly found bilateral hippocampus showing repeatable inter-group differences in cerebral atrophy with aging between the CN and CN2D groups (Left: $F = 47.721$, Right: $F = 30.284$, $p < 0.05/90$, Bonferroni correction). The ROI-wise result could also be validated by the matched validation sub-sample with bilateral hippocampus (Left: $F = 17.998$, Right: $F = 20.027$, $p < 0.05/90$, Bonferroni correction).

3.3. Effects of APOE variants on hippocampal atrophic trajectories

In the full sample dataset, the voxel-wise LME model identified a significant interaction between APOE variants ($\epsilon 4$ carriers vs. noncarriers) and aging on GMV atrophic trajectory in the left hippocampus ($p < 0.05$, FWE correction; Figure 3A). ROI-wise post-hoc analysis based on voxels identified significant APOE and GMV atrophy interaction showed that $\epsilon 4$ carriers suffered a faster accelerated quadratic GMV atrophy in the left hippocampus than the noncarriers ($F = 15.517$, $p < 0.001$; Figure 3B), which was validated by the matched sub-samples ($F = 11.019$, $p < 0.001$; Figure 3C). Similarly, ROI-wise post-hoc analysis based on AAL atlas also demonstrated a faster accelerated quadratic GMV atrophy in $\epsilon 4$ carriers in the left hippocampus than the noncarriers ($F = 9.088$, $p < 0.001$), which was validated by the matched sub-samples ($F = 3.232$, $p = 0.041$).

We further separated participants into four groups (CN& $\epsilon 4$ carriers, CN& $\epsilon 4$ noncarriers, CN2D& $\epsilon 4$ carriers, CN2D& $\epsilon 4$ noncarriers) according to conversion status and APOE genotype and separately outlined their left hippocampal atrophic trajectory. For voxel-wise identified ROI, we found that $\epsilon 4$ carriers showed a faster-accelerated atrophy than $\epsilon 4$ noncarriers in both CN ($F = 8.874$, $p < 0.001$) and CN2D group ($F = 3.000$, $p = 0.050$; Figure 3D), and a similar trend was validated in the validation sub-samples (CN: $F = 2.969$, $p = 0.053$; CN2D: $F = 1.963$, $p = 0.142$; Figure 3E). Meanwhile, $\epsilon 4$ carriers in CN2D group presented a faster atrophic speed than $\epsilon 4$ carriers of CN group in the full cohort ($F = 27.8129$, $p < 0.001$) and validation sub-sample ($F = 8.899$, $p < 0.001$). $\epsilon 4$ noncarriers in CN2D group presented a faster atrophic speed than $\epsilon 4$ carriers of CN group in the full cohort ($F = 13.095$, $p < 0.001$) and validation sub-sample ($F = 3.128$, $p = 0.045$; Figures 3D,E). For AAL atlas, we similarly found that $\epsilon 4$ carriers showed a faster-accelerated atrophy than $\epsilon 4$ noncarriers in both CN ($F = 5.033$, $p = 0.007$) and CN2D group ($F = 4.962$, $p = 0.007$). Meanwhile, $\epsilon 4$ carriers in CN2D group presented a faster atrophic speed than $\epsilon 4$ carriers of CN group in the full cohort ($F = 28.982$, $p < 0.001$). $\epsilon 4$ noncarriers in CN2D group presented a faster atrophic speed than $\epsilon 4$ carriers of CN group in the full cohort ($F = 19.097$, $p < 0.001$). The annual atrophic rates of the left hippocampus demonstrated an upward trend with aging, with the fastest for CN2D& $\epsilon 4$ carriers (0.79% at age 60, 1.81% at age 90), followed by CN2D& $\epsilon 4$ noncarriers (0.77% at age 60, 1.24% at age 90), CN& $\epsilon 4$ carriers (0.22% at age 60, 1.22% at age 90), and slowest for CN& $\epsilon 4$ noncarriers (0.16% at age 60, 0.83% at age 90).

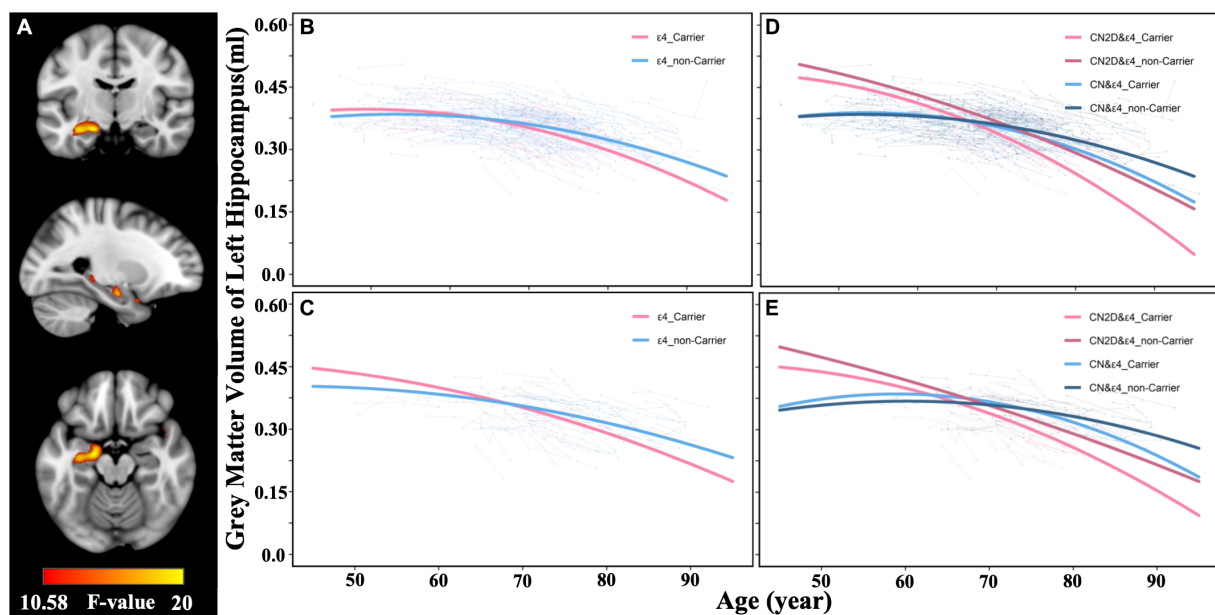


FIGURE 3

Effects of APOE variants on the cerebral longitudinal atrophic trajectories in CN and CN2D groups. (A) represent the voxel-wise differences in GMV atrophic trajectory as a function of aging between APOE $\epsilon 4$ carriers and noncarriers in the full sample dataset. (B,C) represent the atrophic trajectories of the identified left hippocampus in APOE $\epsilon 4$ carriers and noncarriers in the full sample dataset and validation dataset, respectively. (D,E) represent the atrophic trajectories of the left hippocampus in CN& $\epsilon 4$ carriers, CN& $\epsilon 4$ noncarriers, CN2D& $\epsilon 4$ carriers, CN2D& $\epsilon 4$ noncarriers in the full sample dataset, and validation dataset, respectively. CN, persistent cognitive normal; CN2D, cognitive normal to dementia; GMV, gray matter volume.

4. Discussion

This longitudinal neuroimaging study aimed to identify cerebral regions whose atrophic trajectories contribute specifically to the transition from cognitive normal to dementia (CN2D) and outline the effect of APOE variants on cerebral atrophic trajectories during CN2D conversion. We found that CN2D participants had quadratically accelerated atrophy in bilateral hippocampi than persistent CN. Moreover, APOE $\epsilon 4$ carriers had faster-accelerated atrophy in the left hippocampus than $\epsilon 4$ noncarriers in both CN2D and persistent CN, and CN2D $\epsilon 4$ carriers and noncarriers presented a faster atrophic speed than CN $\epsilon 4$ carriers. Finally, APOE $\epsilon 4$ carriers demonstrated faster cognitive decline following aging and hippocampus atrophy. Our findings filled the gap in the mediation of APOE on brain atrophy and cognitive decline during the progression from normal cognition to dementia.

This study is based on the OASIS-3 longitudinal cohort that monitors the natural processes of aging and dementia using multimodal neuroimaging methods. Among the 416 enrolled participants that had normal cognition at the baseline, we found that about 13% (54 cases) of participants converted to dementia during an average follow-up of 6 years. Moreover, based on the data-driven voxel-based morphometry, we found CN2D participants presented faster-accelerated gray matter atrophy following aging than the persistent CN in multiple cerebral regions, especially in the bilateral hippocampi. Previous studies resembled accelerated hippocampal atrophy with aging in normal elders (Crivello et al., 2014; Fraser et al., 2015) and dementia patients (Whitwell, 2010). Moreover, faster hippocampal atrophy had also been reported in AD than in the normal elderly (Jack et al., 1998). Consistent with these studies, based on the OASIS-3 cohort, our findings highlighted the key role of

bilateral hippocampal atrophy in transitioning from cognitively normal people to dementia.

APOE is widely acknowledged as a major risk gene in AD dementia (Gharbi-Meliani et al., 2021; Serrano-Pozo et al., 2021). Early studies have illustrated that APOE $\epsilon 4$ carriers exacerbated gray matter atrophy in the medial temporal lobe and hippocampus in patients with MCI (Schuff et al., 2009; Racine et al., 2018; Abushakra et al., 2020; Zhang et al., 2020) and AD (Li et al., 2016; Saeed et al., 2018; Bilgel and Jedynak, 2019). However, no study has paid attention to the effect of APOE on the trajectory of cerebral atrophy through the whole process from normal cognition to dementia. Our study focused on this issue by voxel-wise modeling the nonlinear atrophy trajectories of the whole brain from cognitively normal to dementia in each APOE variant. We found that APOE $\epsilon 4$ carriers had faster-accelerated atrophy in the left hippocampus than $\epsilon 4$ noncarriers in both CN2D and persistent CN. As we found significant age and gender difference of participants in the full cohort, we demonstrated a further age and gender matched validation sub-sample set in order to minimize age and gender bias. We found that APOE $\epsilon 4$ accelerates the longitudinal hippocampal atrophy in both full cohort and matched sub-samples. Thus, our results based on common results of exploration and validation can be regarded as eliminating the influence of age and gender. In agreement with our findings, multiple recent studies have illustrated APOE $\epsilon 4$ mediated accelerated cerebral atrophy in elder CN (Squarzone et al., 2018; Gorbach et al., 2020; Van Etten et al., 2021; Regy et al., 2022). Besides, APOE $\epsilon 4$ also contributed to faster cerebral atrophy during the conversion from MCI to AD (Wei et al., 2022). Thus, our findings filled the gap regarding the contribution of APOE to cerebral atrophy in the transition from normal cognitive stages to dementia. Moreover, we also found that APOE $\epsilon 4$ carriers demonstrated faster cognitive decline following aging than the

noncarriers, which was supported by early studies reporting APOE $\epsilon 4$ allele presented a significant negative modulative effect on memory, executive functioning, and overall global cognitive ability (Wisdom et al., 2011; Davies et al., 2014).

Our study suggested that bilateral hippocampus was affected during the conversion from CN to dementia while only left hippocampus suffered significant affection with APOE $\epsilon 4$. Asymmetric gray matter volume loss has been reported in previous study that the left hemisphere degenerates faster than the right during Alzheimer disease progression (Thompson et al., 2003). A $n=725$ ADNI cohort analysis published by Shi et al. similarly found APOE $\epsilon 4$ carriers show significant morphological deformation difference in both CN and dementia patients affecting the left hippocampus more than the right relative to noncarriers (Shi et al., 2014). Our findings are corresponding to previous researches.

Alzheimer's disease is characterized by the accumulation of A β plaques and fibrillar tangles containing hyperphosphorylated tau (Selkoe and Hardy, 2016). Though the mechanism between APOE and AD is still under exploration, classic neuropathological theory correlates $\epsilon 4$ carriers with severer A β plaque burden than $\epsilon 4$ noncarriers (Cedazo-Minguez, 2007). Animal experiments also proved that APOE deficiency mice models present decreased amyloid burden in the hippocampus (Ulrich et al., 2018). Furthermore, neuroimaging studies based on A β PET proved that APOE $\epsilon 4$ carriers suffered a higher risk of A β plaque in cognitively normal elders (Jansen et al., 2015) and dementia (Ossenkoppele et al., 2015). Previous studies found that the hippocampus and temporal cortex demonstrated a tight correlation between APOE $\epsilon 4$ mediated A β plaque load and cortical atrophy (Drzezga et al., 2009; Mormino et al., 2009; Chetelat et al., 2010). Besides A β plaque, tau pathology is being increasingly emphasized affecting AD progression. APOE $\epsilon 4$ carriers showed smaller volume and greater tau standardized uptake volume ratio in the hippocampus at baseline while had faster rates of atrophy and faster tau accumulation longitudinally in the hippocampus (Singh et al., 2022). An fMRI study published by Ossenkoppele et al. suggests that tau pathology drives the neurodegeneration through circumscribed brain networks in Alzheimer's disease (Ossenkoppele et al., 2019). They similarly found that tau accumulation in lateral temporal cortex including hippocampus corresponded with cortical thickness and cognitive loss base on a tau-PET study (Ossenkoppele et al., 2019). Animal experiment indicated that the increasing A β plaque deposition leading to loss of large pyramidal neurons in cortical layer 5 and subiculum (Oakley et al., 2006). While microglia-mediated damage is the leading force driving neurodegeneration in a tauopathy mouse model and further leading to gray matter volume loss (Shi et al., 2019). Thus, our findings suggested that APOE $\epsilon 4$ might boost the A β plaque deposition and tau accumulation especially in hippocampus during the full trajectory of AD progression, which further promote hippocampal atrophy and cognitive decline.

We also found that both $\epsilon 4$ carriers and noncarriers with CN2D conversion presented faster accelerated hippocampal atrophy than $\epsilon 4$ carriers with persistent CN, indicating that APOE is not the only risk gene that contributes to the progressive hippocampal atrophy during CN2D conversion. Genome-wide association studies (GWAS) have identified about 40 genetic susceptibility loci of Alzheimer's disease, which are associated with multiple molecular pathways, such as Abeta, tau, immunity, and lipid processing (Jansen et al., 2019; Kunkle et al., 2019; Andrews et al., 2020; Wightman et al., 2021). Moreover, gene-gene and gene-environment interactions also play significant roles in AD conversion and progression (Ghebranious et al., 2011; Burke et al., 2016). Thus, these findings implied that hippocampal atrophy during

the CN2D conversion is not only driven by APOE but also by other latent factors, which should be explored in the future.

Our study is not without limitations for certain. First, longitudinal follow-up sMRI data is difficult to obtain and requires the establishment of a large cohort. Although our study enrolled 416 participants in total, only 54 patients converted from CN to dementia during follow-up. Thus, the deficient sample size in CN2D patients may limit the credibility of this study. Second, due to the lack of tau PET or amyloid PET data in our longitudinal cohort, our study is not able to clarify the direct routine of how APOE allele affecting hippocampus atrophy. Further explanation needs to be combined with multi module image data. Third, our result mainly focuses on a single OASIS3 dataset. The result requires further examination with an independent database to validate its reliability.

5. Conclusion

Based on the OASIS-3 neuroimaging cohort, we found a faster accelerated gray matter atrophy in bilateral hippocampi during the conversion from CN to dementia than during the normal aging process. Moreover, APOE $\epsilon 4$ modulates a faster atrophic speed of the left hippocampus during dementia conversion. Our findings highlight the significance of APOE $\epsilon 4$ in accelerating hippocampal atrophy and the conversion process from CN to Dementia.

Data availability statement

The original contributions presented in the study are included in the article/[Supplementary material](#), further inquiries can be directed to the corresponding authors.

Ethics statement

The studies involving human participants were reviewed and approved by Institutional Review Board of Washington University School of Medicine. The patients/participants provided their written informed consent to participate in this study. Written informed consent was obtained from the individual(s) for the publication of any potentially identifiable images or data included in this article.

Author contributions

YH, WQ, and GZ contributed to the design and implementation of the research. YH written the first draft and revised the final draft. YS, WQ, and GZ provided valuable suggestions for the manuscript. All authors contributed to the article and approved the final version.

Funding

This work was supported by the National Natural Science Foundation of China (82030037, 81871009, 81971599, and 81771818), STI2030-Major Projects (2021ZD0201801), the Translational and Application Project of Brain-inspired and Network Neuroscience on Brain Disorders, Beijing Municipal Health Commission

(11000022T000000444685), and the Tianjin Natural Science Foundation (19JCYBJC25100). Data were provided by OASIS-3 project: Principal Investigators: T. Benzinger, D. Marcus, and J. Morris; NIH P30 AG066444, P50 AG00561, P30 NS09857781, P01 AG026276, P01 AG003991, R01 AG043434, UL1 TR000448, and R01 EB009352. AV-45 doses were provided by Avid Radiopharmaceuticals, a wholly owned subsidiary of Eli Lilly.

Conflict of interest

The authors declare that the research was conducted in the absence of any commercial or financial relationships that could be construed as a potential conflict of interest.

References

- Abushakra, S., Porsteinsson, A. P., Sabbagh, M., Bracoud, L., Schaefer, J., Power, A., et al. (2020). APOE epsilon4/epsilon4 homozygotes with early Alzheimer's disease show accelerated hippocampal atrophy and cortical thinning that correlates with cognitive decline. *Alzheimers Dement.* 6:e12117. doi: 10.1002/trc2.12117
- Andrews, S. J., Fulton-Howard, B., and Goate, A. (2020). Interpretation of risk loci from genome-wide association studies of Alzheimer's disease. *Lancet Neurol.* 19, 326–335. doi: 10.1016/S1474-4422(19)30435-1
- Arbabshirani, M. R., Plis, S., Sui, J., and Calhoun, V. D. (2017). Single subject prediction of brain disorders in neuroimaging: promises and pitfalls. *NeuroImage* 145, 137–165. doi: 10.1016/j.neuroimage.2016.02.079
- Ashburner, J. (2007). A fast diffeomorphic image registration algorithm. *NeuroImage* 38, 95–113. doi: 10.1016/j.neuroimage.2007.07.007
- Belloy, M. E., Napolioni, V., and Greicius, M. D. (2019). A quarter century of APOE and Alzheimer's disease: Progress to date and the path forward. *Neuron* 101, 820–838. doi: 10.1016/j.neuron.2019.01.056
- Bernal-Rusiel, J. L., Greve, D. N., Reuter, M., Fischl, B., and Sabuncu, M. R. Alzheimer's Disease Neuroimaging Initiative (2013). Statistical analysis of longitudinal neuroimaging data with linear mixed effects models. *NeuroImage* 66, 249–260. doi: 10.1016/j.neuroimage.2012.10.065
- Bilgel, M., and Jernigan, B. M. (2019). Predicting time to dementia using a quantitative template of disease progression. *Alzheimers Dement. (Amst)*. 11, 205–215. doi: 10.1016/j.dadm.2019.01.005
- Buckner, R. L. (2004). Memory and executive function in aging and AD: multiple factors that cause decline and reserve factors that compensate. *Neuron* 44, 195–208. doi: 10.1016/j.neuron.2004.09.006
- Burggren, A. C., Zeineh, M. M., Ekstrom, A. D., Braskie, M. N., Thompson, P. M., Small, G. W., et al. (2008). Reduced cortical thickness in hippocampal subregions among cognitively normal apolipoprotein E ε4 carriers. *NeuroImage* 41, 1177–1183. doi: 10.1016/j.neuroimage.2008.03.039
- Burke, S. L., Maramaldi, P., Cadet, T., and Kukull, W. (2016). Associations between depression, sleep disturbance, and apolipoprotein E in the development of Alzheimer's disease: dementia. *Int. Psychogeriatr.* 28, 1409–1424. doi: 10.1017/S1041610216000405
- Cedazo-Minguez, A. (2007). Apolipoprotein E and Alzheimer's disease: molecular mechanisms and therapeutic opportunities. *J. Cell. Mol. Med.* 11, 1227–1238. doi: 10.1111/j.1582-4934.2007.00130.x
- Chetelat, G., Villemagne, V. L., Bourgeat, P., Pike, K. E., Jones, G., Ames, D., et al. (2010). Relationship between atrophy and beta-amyloid deposition in Alzheimer disease. *Ann. Neurol.* 67, 317–324. doi: 10.1002/ana.21955
- Crivello, F., Tzourio-Mazoyer, N., Tzourio, C., and Mazoyer, B. (2014). Longitudinal assessment of global and regional rate of grey matter atrophy in 1,172 healthy older adults: modulation by sex and age. *PLoS One* 9:e114478. doi: 10.1371/journal.pone.0114478
- Davies, G., Harris, S. E., Reynolds, C. A., Payton, A., Knight, H. M., Liewald, D. C., et al. (2014). A genome-wide association study implicates the APOE locus in nonpathological cognitive ageing. *Mol. Psychiatry* 19, 76–87. doi: 10.1038/mp.2012.159
- Drzega, A., Grimmer, T., Henriksen, G., Muhlau, M., Perneczky, R., Miederer, I., et al. (2009). Effect of APOE genotype on amyloid plaque load and gray matter volume in Alzheimer disease. *Neurology* 72, 1487–1494. doi: 10.1212/WNL.0b013e3181a2e8d0
- Fraser, M. A., Shaw, M. E., and Cherbuin, N. (2015). A systematic review and meta-analysis of longitudinal hippocampal atrophy in healthy human ageing. *NeuroImage* 112, 364–374. doi: 10.1016/j.neuroimage.2015.03.035

Publisher's note

All claims expressed in this article are solely those of the authors and do not necessarily represent those of their affiliated organizations, or those of the publisher, the editors and the reviewers. Any product that may be evaluated in this article, or claim that may be made by its manufacturer, is not guaranteed or endorsed by the publisher.

Supplementary material

The Supplementary material for this article can be found online at: <https://www.frontiersin.org/articles/10.3389/fnagi.2023.1158579/full#supplementary-material>

Gharbi-Meliani, A., Dugravot, A., Sabia, S., Regy, M., Faysos, A., Schnitzler, A., et al. (2021). The association of APOE epsilon4 with cognitive function over the adult life course and incidence of dementia: 20 years follow-up of the Whitehall II study. *Alzheimers Res. Ther.* 13:5. doi: 10.1186/s13195-020-00740-0

Ghebranious, N., Mukesh, B., Giampietro, P. F., Glurich, I., Mickel, S. F., Waring, S. C., et al. (2011). A pilot study of gene/gene and gene/environment interactions in Alzheimer disease. *Clin. Med. Res.* 9, 17–25. doi: 10.3121/cmr.2010.894

Gorbach, T., Pudas, S., Bartes-Faz, D., Brandmaier, A. M., Duzel, S., Henson, R. N., et al. (2020). Longitudinal association between hippocampus atrophy and episodic-memory decline in non-demented APOE epsilon4 carriers. *Alzheimers Dement.* 12:e12110. doi: 10.1002/dad2.12110

Hanck, C., Arnold, M., and Gerber, A. (2019). Schmelzer MJUoD-E. 2019. *Introduction to Econometrics with R*, pp. 1–9.

Jack, C. R., Petersen, R. C., Xu, Y., O'Brien, P. C., Smith, G. E., Ivnik, R. J., et al. (1998). Rate of medial temporal lobe atrophy in typical aging and Alzheimer's disease. *Neurology* 51, 993–999. doi: 10.1212/wnl.51.4.993

Jack, C. R., Shiung, M. M., Weigand, S. D., O'Brien, P. C., Gunter, J. L., Boeve, B. F., et al. (2005). Brain atrophy rates predict subsequent clinical conversion in normal elderly and amnesic MCI. *Neurology* 65, 1227–1231. doi: 10.1212/01.wnl.0000180958.22678.91

Jansen, W. J., Ossenkoppele, R., Knol, D. L., Tijms, B. M., Scheltens, P., Verhey, F. R., et al. (2015). Prevalence of cerebral amyloid pathology in persons without dementia: a meta-analysis. *JAMA* 313, 1924–1938. doi: 10.1001/jama.2015.4668

Jansen, I. E., Savage, J. E., Watanabe, K., Bryois, J., Williams, D. M., Steinberg, S., et al. (2019). Genome-wide meta-analysis identifies new loci and functional pathways influencing Alzheimer's disease risk. *Nat. Genet.* 51, 404–413. doi: 10.1038/s41588-018-0311-9

Kanekiyo, T., Xu, H., and Bu, G. (2014). ApoE and Abeta in Alzheimer's disease: accidental encounters or partners? *Neuron* 81, 740–754. doi: 10.1016/j.neuron.2014.01.045

Kunkle, B. W., Grenier-Boley, B., Sims, R., Bis, J. C., Damotte, V., Naj, A. C., et al. (2019). Genetic meta-analysis of diagnosed Alzheimer's disease identifies new risk loci and implicates Abeta, tau, immunity and lipid processing. *Nat. Genet.* 51, 414–430. doi: 10.1038/s41588-019-0358-2

Li, B., Shi, J., Gutman, B. A., Baxter, L. C., Thompson, P. M., Caselli, R. J., et al. (2016). Influence of APOE genotype on hippocampal atrophy over time - an N=1925 surface-based ADNI study. *PLoS One* 11:e0152901. doi: 10.1371/journal.pone.0152901

Lian, C., Liu, M., Zhang, J., and Shen, D. (2020). Hierarchical fully convolutional network for joint atrophy localization and Alzheimer's disease diagnosis using structural MRI. *IEEE Trans. Pattern Anal. Mach. Intell.* 42, 880–893. doi: 10.1109/TPAMI.2018.2889096

Lu, P. H., Thompson, P. M., Leow, A., Lee, G. J., Lee, A., Yanovsky, I., et al. (2011). Apolipoprotein E genotype is associated with temporal and hippocampal atrophy rates in healthy elderly adults: a tensor-based morphometry study. *J. Alzheimers Dis.* 23, 433–442. doi: 10.3233/JAD-2010-101398

Mahoney-Sanchez, L., Belaidi, A. A., Bush, A. I., and Ayton, S. (2016). The complex role of apolipoprotein E in Alzheimer's disease: an overview and update. *J. Mol. Neurosci.* 60, 325–335. doi: 10.1007/s12031-016-0839-z

Mormino, E. C., Kluth, J. T., Madison, C. M., Rabinovici, G. D., Baker, S. L., Miller, B. L., et al. (2009). Episodic memory loss is related to hippocampal-mediated beta-amyloid deposition in elderly subjects. *Brain* 132, 1310–1323. doi: 10.1093/brain/awn320

- Oakley, H., Cole, S. L., Logan, S., Maus, E., Shao, P., Craft, J., et al. (2006). Intraneuronal beta-amyloid aggregates, neurodegeneration, and neuron loss in transgenic mice with five familial Alzheimer's disease mutations: potential factors in amyloid plaque formation. *J. Neurosci.* 26, 10129–10140. doi: 10.1523/JNEUROSCI.1202-06.2006
- Ossenkopppele, R., Iaccarino, L., Schonhaut, D. R., Brown, J. A., La Joie, R., O'Neil, J. P., et al. (2019). Tau covariance patterns in Alzheimer's disease patients match intrinsic connectivity networks in the healthy brain. *Neuroimage Clin.* 23:101848. doi: 10.1016/j.nicl.2019.101848
- Ossenkopppele, R., Jansen, W. J., Rabinovici, G. D., Knol, D. L., van der Flier, W. M., van Berckel, B. N., et al. (2015). Prevalence of amyloid PET positivity in dementia syndromes: a meta-analysis. *JAMA* 313, 1939–1949. doi: 10.1001/jama.2015.4669
- Ossenkopppele, R., Smith, R., Ohlsson, T., Strandberg, O., Mattsson, N., Insel, P. S., et al. (2019). Associations between tau, Aβeta, and cortical thickness with cognition in Alzheimer disease. *Neurology* 92, e601–e612. doi: 10.1212/WNL.00000000000006875
- Pini, L., Pievani, M., Bocchetta, M., Altomare, D., Bosco, P., Cavedo, E., et al. (2016). Brain atrophy in Alzheimer's disease and aging. *Ageing Res. Rev.* 30, 25–48. doi: 10.1016/j.arr.2016.01.002
- Racine, A. M., Brickhouse, M., Wolk, D. A., and Dickerson, B. C. Alzheimer's Disease Neuroimaging Initiative (2018). The personalized Alzheimer's disease cortical thickness index predicts likely pathology and clinical progression in mild cognitive impairment. *Alzheimers Dement.* 10, 301–310. doi: 10.1016/j.dadm.2018.02.007
- Radua, J., Canales-Rodriguez, E. J., Pomarol-Clotet, E., and Salvador, R. (2014). Validity of modulation and optimal settings for advanced voxel-based morphometry. *NeuroImage* 86, 81–90. doi: 10.1016/j.neuroimage.2013.07.084
- Rathore, S., Habes, M., Iftikhar, M. A., Shacklett, A., and Davatzikos, C. (2017). A review on neuroimaging-based classification studies and associated feature extraction methods for Alzheimer's disease and its prodromal stages. *NeuroImage* 155, 530–548. doi: 10.1016/j.neuroimage.2017.03.057
- Regy, M., Dugravot, A., Sabia, S., Fayosse, A., Mangin, J. F., Chupin, M., et al. (2022). Association of APOE ε4 with cerebral gray matter volumes in non-demented older adults: the MEMENTO cohort study. *NeuroImage* 250:118966. doi: 10.1016/j.neuroimage.2022.118966
- Saeed, U., Desmarais, P., and Masellis, M. (2021). The APOE ε4 variant and hippocampal atrophy in Alzheimer's disease and Lewy body dementia: a systematic review of magnetic resonance imaging studies and therapeutic relevance. *Expert. Rev. Neurother.* 21, 851–870. doi: 10.1080/14737175.2021.1956904
- Saeed, U., Mirza, S. S., MacIntosh, B. J., Herrmann, N., Keith, J., Ramirez, J., et al. (2018). APOE-ε4 associates with hippocampal volume, learning, and memory across the spectrum of Alzheimer's disease and dementia with Lewy bodies. *Alzheimers Dement.* 14, 1137–1147. doi: 10.1016/j.jalz.2018.04.005
- Scheltens, P., De Strooper, B., Kivipelto, M., Holstege, H., Chételat, G., Teunissen, C. E., et al. (2021). Alzheimer's disease. *Lancet* 397, 1577–1590. doi: 10.1016/s0140-6736(20)32205-4
- Schuff, N., Woerner, N., Boreta, L., Kornfield, T., Shaw, L. M., Trojanowski, J. Q., et al. (2009). MRI of hippocampal volume loss in early Alzheimer's disease in relation to ApoE genotype and biomarkers. *Brain* 132, 1067–1077. doi: 10.1093/brain/awp007
- Selkoe, D. J., and Hardy, J. (2016). The amyloid hypothesis of Alzheimer's disease at 25 years. *EMBO Mol. Med.* 8, 595–608. doi: 10.15252/emmm.201606210
- Serrano-Pozo, A., Das, S., and Hyman, B. T. (2021). APOE and Alzheimer's disease: advances in genetics, pathophysiology, and therapeutic approaches. *Lancet Neurol.* 20, 68–80. doi: 10.1016/s1474-4422(20)30412-9
- Shaffer, J. P. (1995). Multiple hypothesis testing. *Ann. Rev. Psychol.* 46, 561–584. doi: 10.1146/annurev.ps.46.020195.003021
- Shi, J., Lepore, N., Gutman, B. A., Thompson, P. M., Baxter, L. C., Caselli, R. J., et al. (2014). Genetic influence of apolipoprotein E4 genotype on hippocampal morphometry: an N = 725 surface-based Alzheimer's disease neuroimaging initiative study. *Hum. Brain Mapp.* 35, 3903–3918. doi: 10.1002/hbm.22447
- Shi, Y., Manis, M., Long, J., Wang, K., Sullivan, P. M., Remolina Serrano, J., et al. (2019). Microglia drive APOE-dependent neurodegeneration in a tauopathy mouse model. *J. Exp. Med.* 216, 2546–2561. doi: 10.1084/jem.20190980
- Singh, N. A., Tosakulwong, N., Graff-Radford, J., Machulda, M. M., Pham, N. T. T., Sintini, I., et al. (2022). APOE ε4 influences medial temporal atrophy and tau deposition in atypical Alzheimer's disease. *Alzheimers Dement.* 2022:12711. doi: 10.1002/alz.12711
- Squarzoni, P., Duran, F. L. S., Busatto, G. F., and Alves, T. (2018). Reduced gray matter volume of the thalamus and hippocampal region in elderly healthy adults with no impact of APOE ε4: a longitudinal voxel-based morphometry study. *J. Alzheimers Dis.* 62, 757–771. doi: 10.3233/JAD-161036
- Tabatabaei-Jafari, H., Shaw, M. E., Walsh, E., and Cherbuin, N. Alzheimer's Disease Neuroimaging Initiative (2019). Regional brain atrophy predicts time to conversion to Alzheimer's disease, dependent on baseline volume. *Neurobiol. Aging* 83, 86–94. doi: 10.1016/j.neurobiolaging.2019.08.033
- Thompson, P. M., Hayashi, K. M., de Zubicaray, G., Janke, A. L., Rose, S. E., Semple, J., et al. (2003). Dynamics of gray matter loss in Alzheimer's disease. *J. Neurosci.* 23, 994–1005. doi: 10.1523/JNEUROSCI.23-03-00994.2003
- Tzourio-Mazoyer, N., Landeau, B., Papathanassiou, D., Crivello, F., Etard, O., Delcroix, N., et al. (2002). Automated anatomical labeling of activations in SPM using a macroscopic anatomical parcellation of the MNI MRI single-subject brain. *NeuroImage* 15, 273–289. doi: 10.1006/nimg.2001.0978
- Ulrich, J. D., Ulland, T. K., Mahan, T. E., Nystrom, S., Nilsson, K. P., Song, W. M., et al. (2018). ApoE facilitates the microglial response to amyloid plaque pathology. *J. Exp. Med.* 215, 1047–1058. doi: 10.1084/jem.20171265
- Van Etten, E. J., Bharadwaj, P. K., Hishaw, G. A., Huentelman, M. J., Trouard, T. P., Grilli, M. D., et al. (2021). Influence of regional white matter hyperintensity volume and apolipoprotein E ε4 status on hippocampal volume in healthy older adults. *Hippocampus* 31, 469–480. doi: 10.1002/hipo.23308
- Veitch, D. P., Weiner, M. W., Aisen, P. S., Beckett, L. A., Cairns, N. J., Green, R. C., et al. (2019). Understanding disease progression and improving Alzheimer's disease clinical trials: recent highlights from the Alzheimer's disease Neuroimaging initiative. *Alzheimers Dement.* 15, 106–152. doi: 10.1016/j.jalz.2018.08.005
- Wei, X., Du, X., Xie, Y., Suo, X., He, X., Ding, H., et al. (2022). Mapping cerebral atrophic trajectory from amnesic mild cognitive impairment to Alzheimer's disease. *Cereb. Cortex* 33, 1310–1327. doi: 10.1093/cercor/bhac137
- Whitwell, J. L. (2010). Progression of atrophy in Alzheimer's disease and related disorders. *Neurotox. Res.* 18, 339–346. doi: 10.1007/s12640-010-9175-1
- Wightman, D. P., Jansen, I. E., Savage, J. E., Shadrin, A. A., Bahrami, S., Holland, D., et al. (2021). A genome-wide association study with 1,126,563 individuals identifies new risk loci for Alzheimer's disease. *Nat. Genet.* 53, 1276–1282. doi: 10.1038/s41588-021-00921-z
- Wisdom, N. M., Callahan, J. L., and Hawkins, K. A. (2011). The effects of apolipoprotein E on non-impaired cognitive functioning: a meta-analysis. *Neurobiol. Aging* 32, 63–74. doi: 10.1016/j.neurobiolaging.2009.02.003
- Zhang, C., Kong, M., Wei, H., Zhang, H., Ma, G., Ba, M., et al. (2020). The effect of ApoE ε4 on clinical and structural MRI markers in prodromal Alzheimer's disease. *Quant. Imaging Med. Surg.* 10, 464–474. doi: 10.21037/qims.2020.01.14